ground water

Radial Flow Permeability Testing of an Argillaceous Limestone

by A.P.S. Selvadurai[1] and L. Jenner[2]

Abstract

Argillaceous Lindsay limestone is the geologic storage formation that will be encountered at the site for the construction of a deep ground repository in Ontario, Canada, for the storage of low to intermediate level nuclear waste. The permeability of the Lindsay limestone is a key parameter that will influence the long-term movement of radionuclides from the repository to the geosphere. This paper describes the use of both steady-state and transient radial flow laboratory tests to determine the permeability of this argillaceous limestone. The interpretation of the tests is carried out using both analytical results and computational models of flow problems that exhibit radial symmetry. The results obtained from this research investigation are compared with the data available in the literature for similar argillaceous limestones mainly found in the Lindsay (Cobourg) formation. The experiments give permeabilities in the range of 1.0×10^{-22} to 1.68×10^{-19} m^2 for radial flows that are oriented along bedding planes under zero axial stress. The factors influencing transient pulse tests in particular and the interpretation of the results are discussed.

Introduction

Permeability is a measure of fluid transport through the continuously connected pore space of a porous medium. It is an important property for problems in the engineering geosciences ranging from hydrogeology of water resources management to contaminant transport. Recently, the importance of permeability in porous media has been highlighted in geoenvironmental endeavors associated with geological sequestration of CO_2, geothermal energy extraction, groundwater contamination by stored mine tailings and in the geologic disposal of hazardous materials such as nuclear wastes (see e.g., Chapman and McKinley 1987; Bear et al. 1993; Selvadurai and Nguyen 1996; Bachu and Adams 2003; Alonso et al. 2005; Selvadurai 2002, 2006). This paper deals with the laboratory evaluation of the permeability of the argillaceous Lindsay limestone found in southern Ontario, Canada. This limestone formation has been identified as the host rock for the construction of a geologic repository for storing low and intermediate level nuclear waste (Mazurek 2004; Lam et al. 2007; Gartner Lee Ltd. 2008; Selvadurai et al. 2011). This paper describes both steady-state and transient permeability tests that were conducted on four hollow cylindrical samples of the Lindsay limestone in order to estimate their in-plane permeability characteristics under unconfined conditions. The details of the experimental procedures involving radial flow test results are documented by Jenner (2011).

[1]Corresponding author: Civil Engineering and Applied Mechanics, McGill University, 817 Sherbrooke Street West, Montrea, QC H3A 2K6, Canada; (1) 514-398-6672; fax: (1) 514-398-7361; patrick.selvadurai@mcgill.ca

[2]Civil Engineering and Applied Mechanics, McGill University, 817 Sherbrooke Street West, Montrea, QC H3A 2K6, Canada.

Received August 2011, accepted February 2012.

doi: 10.1111/j.1745-6584.2012.00932.x

Theoretical Background

The techniques used to measure the permeability of porous intact rocks are largely dictated by some prior indication of the range of permeabilities identified with the type of rock. The two basic categories of tests used to measure permeability are either steady-state tests or transient tests. In both types of tests, however, it is implicit that the flow in the pore space is governed by Darcy's law. Steady-state tests are advocated for rocks through which a steady measurable flow rate can be established without damaging the sample. Steady-state tests have been successfully used for testing low permeability porous materials (see e.g., Bernaix 1969; Daw 1971; Trimmer et al. 1980; Heystee and Roegiers 1981; Hearn and Mills 1991; Selvadurai and Carnaffan 1997; Selvadurai et al. 2005; Selvadurai and Głowacki 2008; Selvadurai and Selvadurai 2007, 2010). In certain rocks with very low permeability (e.g., permeability in the range of 10^{-23} to 10^{-19} m^2), the steady flow rates that can be induced without damaging the sample are extremely small and such geologic materials require the use of transient techniques for measuring their permeability. The steady-state test involves the application of a constant hydraulic gradient across known boundaries of a sample and measures the corresponding fluid flow rate. The advantage of the steady-state test is that very few additional parameters, other than the geometry of the test configuration and the hydraulic head boundary conditions, are needed to interpret the test data. When the datum head can be neglected in comparison to the pressure head $p(\mathbf{x})/\gamma_w$, where $p(\mathbf{x})$ is the pressure field, $\mathbf{x}$ a position vector, and γ_w the unit weight of water, the partial differential equation governing steady flow is Laplace's equation given by

$$\nabla^2 p(\mathbf{x}) = 0 \tag{1}$$

where ∇^2 is Laplace's operator. The governing Equation 1 has to be solved for appropriate Dirichlet and/or Neumann boundary conditions relevant to the flow domain (Selvadurai 2000). The estimation of permeability is linked to the geometry of the flow domain and the measured flow rate under the fluid potential differential across a tested region. As is evident, no other parameter is needed to estimate the hydraulic conductivity of the porous medium, and the permeability is estimated through knowledge of the viscosity of water and its unit weight, both of which are reasonably well known for the temperature and pressures associated with the test. One of the drawbacks of conducting steady-state tests in low permeability geomaterials is the extended duration required to attain steady-state conditions. Therefore, fluid transport characteristics of very low permeability rocks are measured by using transient flow techniques, which involves the application of a pressure pulse to a fixed region of a fluid volume that maintains contact with the surface of a saturated flow domain. The simplest form of the partial differential equation governing the diffusion of the time- and position-dependent fluid pressure $p(\mathbf{x}, t)$ within the fluid-saturated porous medium is given by (see e.g., Barenblatt et al. 1990; Selvadurai 2000)

$$\left(\frac{K}{\mu(n^* C_w + C_{eff})}\right)\nabla^2 p(\mathbf{x}, t) = \frac{\partial p(\mathbf{x}, t)}{\partial t} \tag{2}$$

where K is the permeability of the porous medium, μ the dynamic viscosity of the pore fluid, n^* the porosity, and C_w and C_{eff} are, respectively, the compressibilities of the pore fluid and the porous skeleton. Other contributions, including the compressibility of the solid grains (C_s), can be included in the description of the overall compressibility of the system (Brace et al. 1968). The partial differential Equation 2 needs to be solved for the specific Dirichlet and Neumann boundary conditions applicable to the test configuration as well as the initial condition governing the pressure field in the domain at the start of a test. It is clear that the solution of Equation 2, which is used to determine the permeability K, will depend on other factors, including the porosity of the porous medium and the compressibilities of the pore fluid and the porous skeleton. In a laboratory context, the uniaxial flow hydraulic pulse testing of low permeability geomaterials is extensively documented in the works of Brace et al. (1968), Hsieh et al. (1981) and others, and an extensive account of developments in this area is also given by Selvadurai et al. (2005) and Selvadurai (2009).

This paper deals with the radial flow hydraulic pulse testing of the argillaceous Lindsay limestone. Radial flow pulse tests have also been used extensively in *well testing* associated with hydrogeological investigations (Cooper et al. 1967; Bredehoeft and Papadopulos 1980) and the techniques can be adapted in the laboratory as radial flow transient tests. Selvadurai and Carnaffan (1997) applied radial flow hydraulic pulses to determine the permeability of cement grout and Selvadurai et al. (2005) used the same technique to determine the permeability of cylinders of Barre Granite. In this research, the boundary conditions associated with the experimental simulation of axisymmetric flow pulse tests are not amenable to convenient mathematical modeling; for this reason, the experiment involving axisymmetric transient flow is examined using a computational approach.

The Lindsay Limestone and Experimental Procedures

Lindsay limestone is a mottled light to dark heterogeneous rock. This hard, nodular limestone is classified as argillaceous and contains numerous small invertebrate fossils as well as thin shale layers usually less than a centimeter thick. The articles by Raven et al. (1992), Golder Associates (2003), Mazurek (2004), and Gartner Lee Ltd. (2008) give comprehensive accounts of the composition of Lindsay limestone. The rock is composed of two primary species; the lighter carbonate nodular rock and the darker agillacaceous material.

Sample Preparation

Blocks of Lindsay limestone were obtained from the Saint Mary's Quarry in Bowmanville, Ontario, Canada. The limestone at the depth of recovery of the blocks is assumed to have geologic features similar to those found in cores recovered at a depth of 680 m, which is approximately the anticipated depth of the proposed deep ground repository (DGR) (Gartner Lee Ltd. 2008). The recovered blocks were cut into two large cubes (Figure 1)

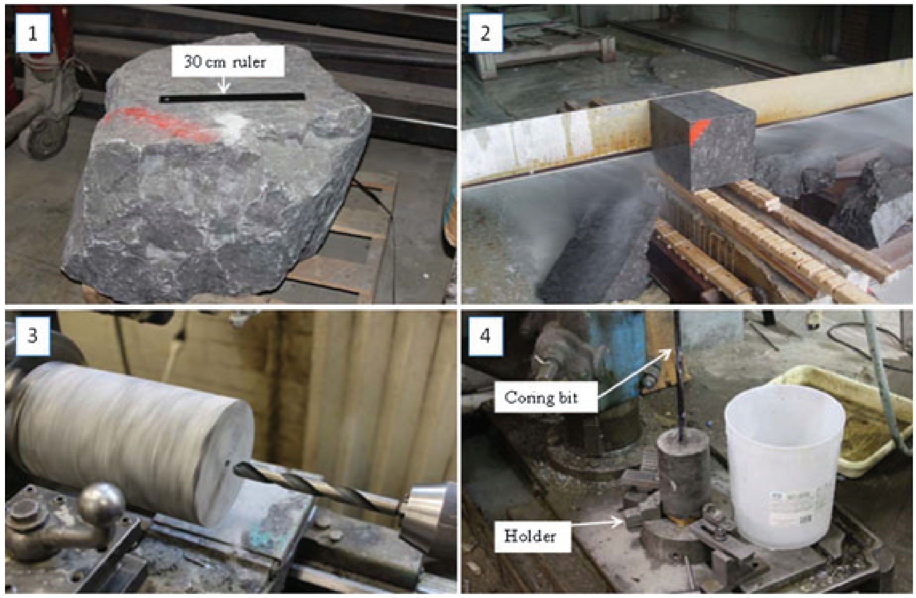

Figure 1. Sample preparation. (1) Original block, (2) preparation of cuboidal specimen, (3) creating dimple in sample to facilitate coring, and (4) coring inner cavity.

to facilitate the coring of samples. The DGR Site Core was cored deep within the actual proposed host rock horizon. Three samples from the quarried block and a DGR Site Core of diameter of approximately 106.8 mm and lengths between 116.8 and 173.6 mm were tested. The inner cavity for the radial flow experiments was created using a 12.7 mm diameter coring bit. The general techniques adopted in the preparation of the cubical block and the cylindrical test specimens are shown in Figure 1. Since the inner cavity was pressurized during the tests, the central cavity was sealed at the open ends, using fittings with valves that were epoxy sealed to the surface of the rock. The cylindrical samples chosen for the experiments exhibited evidence of stratification along the bedding plane. Previous research investigations (Vilks and Miller 2007; Gartner Lee Ltd. 2008) showed an order of magnitude difference in the permeability orthotropy.

The Experimental Facility

The fluid-saturated sample, with cavity ends sealed, was placed in a water bath that was maintained at a constant temperature of 21° C. The lower entry point of the central cavity (Figure 2) was used as the water inlet, which prevents trapping of any excess air. The upper exit point of the sealed cavity was connected to a pressure transducer (Honeywell Transducer/Sensotech LM, Columbus, Ohio) in order to monitor the cavity pressures. The lower water entry point was connected to a Quizix pump (Model QX-6000-HC, Vindum Engineering, California) which provided the de-aired, filtered water; no attempt was made to match the chemical composition of water used in the experiments to the in situ groundwater. The experimental configuration involved the pressurization of the cylindrical cavity located along the axis of the sample, with real time pressure vs. time displayed for the transient hydraulic pulse test (Jenner 2011).

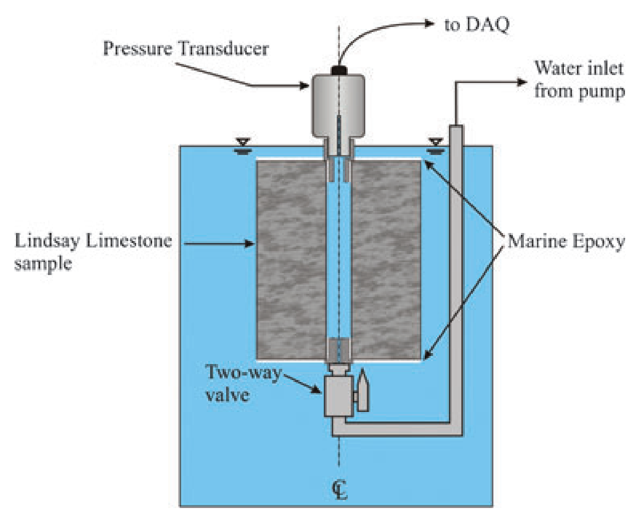

Figure 2. Cross-section of a typical test specimen.

Theoretical and Computational Modeling

In this section, we briefly review the theoretical and computational approaches that have been adopted for the solution of the steady-state and transient problems related to both radial and axisymmetric flows for various experimental configurations. More complete discussions of the topics can be found in the seminal articles cited previously.

Steady-State Flow

The geometrical configuration of the purely radial flow problem involves the solution of Laplace's Equation 1 expressed in radial coordinates and subject to the boundary conditions

$$p(b) = p_b;\ p(a) = p_a \tag{3}$$

where p_a and p_b are, respectively, the pressures induced at the inner boundary $r = a$ and the outer boundary $r = b$ during the application of a steady outward flow rate Q through the cylindrical sample of length H_0. The solution of the governing ordinary differential equation can be used to develop an expression from which the permeability can be calculated (see also Thiem 1906; Muskat and Wyckoff 1946; Ferris et al. 1962). We have

$$K = \frac{Q\mu \log_e(b/a)}{2\pi H_0(p_a - p_b)}. \tag{4}$$

In the experimental configuration the exterior pressure p_b is neglected in comparison to the interior pressure p_a. This solution was also used to calibrate the accuracy of computational simulations of the steady-state problem.

Transient Pulse Test

A convenient analytical approach for the solution of the partial differential Equation 2 is feasible only when flow in the porous domain is purely radial. The mathematical formulation of the transient radial flow problem has been described in several of the references cited previously and the salient results are summarized for completeness and for ease of discussion. The analysis of the solution to the initial boundary value problem governing the decay of the pressure pulse from the cylindrical cavity to the fluid-saturated porous medium of infinite extent can be gleaned from the results for the analogous transient heat conduction problem (Carslaw and Jaeger 1959), and convenient expressions are given by Bredehoeft et al. (1966), Cooper et al. (1967) and Bredehoeft and Papadopulos (1980). The study by Selvadurai et al. (2005) also gives a complete analysis and indicates the range of parameters that warrant the treatment of the flow domain as a fluid-saturated domain of infinite extent. For such a flow domain, the time-dependent decay of a pressure pulse of intensity p_0, which is applied as a Dirac delta function of time within the central cavity, is given by

$$\frac{p(t)}{p_0} = \frac{8\alpha}{\pi^2}\int_0^\infty \frac{\exp(-\beta u^2/\alpha)}{u f(u,\alpha)}\mathrm{d}u \tag{5}$$

where

$$f(u,\alpha) = [uJ_0(u) - 2\alpha J_1(u)]^2 - [uY_0(u) - 2\alpha Y_1(u)]^2 \tag{6}$$

and J_0 and J_1 are, respectively, the zeroth-order and first-order Bessel functions of the first kind and Y_0 and Y_1 are the zeroth-order and first-order Bessel functions of the second kind, respectively. Also in Equation 5, the nondimensional parameters α and β are given by

$$\alpha = \frac{\pi a^2 H_0}{V_\mathrm{w}}\left(n^* + \frac{C_\mathrm{eff}}{C_\mathrm{w}}\right); \beta = \frac{\pi K H_0 t}{\mu V_\mathrm{w} C_\mathrm{w}} \tag{7}$$

where V_w is the volume of the fluid within the cavity and the connector lines that is subjected to the pressure increase. As formulated above, all the material, physical, and geometric parameters in the transient decay of the pressure pulse within the pressurized cavity are known, except for the permeability of the porous medium K. A match between the experimental pressure decay curve and a theoretical result can be sought by varying the permeability K. Tables of values of the integral (Equation 5) for a range of α and β are given by Cooper et al. (1967) and Bredehoeft and Papadopulos (1980). The integral in Equation 5 can be conveniently evaluated for specific choices of the nondimensional parameters α and β using standard mathematical software such as Mathematica™ (Wolfram Research, Champaign, Illinois) and Maple™ (Maplesoft, Ontario, Canada).

Computational Modeling of Steady-State Flow

Computational modeling of the steady-state flow problem was performed using the computational multiphysics code COMSOL™ (COMSOL Inc., Burlington, Massachusetts). The accuracy of the code has been extensively verified for both two-dimensional and three-dimensional problems (Selvadurai and Selvadurai 2007, 2010) and the details are not repeated here. It is sufficient to note that the computational result for the steady-state flow rate in Equation 4 can be calculated to within an accuracy of 0.04%. The mesh refinement needed to achieve this result is extended to computational simulations of both transient radial flow and transient axisymmetric flow problems. If air is present in the pressurized fluid-filled cavity, this can lead to an underestimation of the permeability. The presence of air can lead to errors in the estimation of permeability through either the alterations in the effective compressibility of the fluid or possible pore clogging in the event any dissolved air is released from the depressurizing fluid within the cavity and obstructs the surface of the cavity.

Computational Modeling of Transient Flow

Computational modeling of the transient pulse tests was performed using the COMSOL code. Transient pulse tests are best modeled by adopting an artifice to simulate the central pressurized region. The modeling of the central pressurized fluid-filled cavity, to create the transient effects of pressure diffusion, was accomplished by simulating the entire cavity as a porous medium with a permeability and porosity substantially larger than that the tested geologic medium ($K = 1 \times 10^{-14}$ m^2 and $n = 1$). This computational approach for simulating hydraulic pulse tests was used by Selvadurai (2010). (It should also be noted that in the context of the treatment of a radial flow pulse test Bredehoeft et al. (1966) used an electrical analog technique to examine a related problem.) The boundary of the fluid domain is maintained fixed to ensure that there is no expansion of the fluid domain, which could contribute to pressure loss. When fluid pressures are applied to the fluid cavity region, the fluid pressures in the rock specimen will be zero, corresponding to the initial value assigned in the solution of the governing partial differential Equation 2. This results in a discontinuity in the pressure field between the fluid cavity and the saturated geologic medium. Although this can be handled relatively conveniently in the analytical solution of the problem, the computational modeling requires that sufficient mesh refinement be provided at the regions close to the saturated, porous medium-pressurized, fluid-filled cavity interface to allow for oscillation-free transmission of the pressure pulse from the pressurized cavity region to the porous fluid-saturated geologic material. Ideally, the mesh refinement between these regions should be based on adaptive discretization algorithms in space and time. Because such options are not provided for in the COMSOL code, the accuracy of the computational modeling of the transient pressure pulse decay in the pressurized cavity is established by mesh refinement applied to both the fluid domain and the fluid-saturated porous region at either side of the interface between the two regions. The nodes at the boundary were set for each sub-domain and these were used to discretize each sub-domain. The finite element discretizations use Lagrangian (C_0 continuity) linear quadrilateral axisymmetric elements. The parameters used in the analytical and computational modeling correspond to the following: $a = 0.00684$ m; $b = 0.0534$ m; $H_0 = 0.11684$ m; $V_w = 22.036 \times 10^{-6}$ m^3; $C_w = 4.54 \times 10^{-10}$ m^2/kN; $C_{eff} = 7.22 \times 10^{-8}$m^2/kN; $n^* = 0.01$; and $K = 1 \times 10^{-20}$ m^2 (these values correspond to the geometrical configuration of the experimental arrangement and typical properties applicable to the Lindsay limestone). The dynamic fluid viscosity for the temperature in the tests (~21° C) is obtained from the results given by White (1986): that is, $\mu = 10^{-6}$ KN sec/m^2. The maximum percentage difference between the analytical and computational results for the pressure decay in the pressurized region is 0.11% for 350-s simulations.

The computational modeling of the actual experimental configuration differs from the purely radial flow problem in that, due to the epoxy sealing techniques used in the experiments, the flow pattern is no longer purely radially symmetric (i.e., spatially dependent only on the radial coordinate) but axisymmetric (spatially dependent on both the radial coordinate r and axial coordinate z). Figure 3 illustrates the boundary condition used for all laboratory tests; the computational modeling therefore has to take into consideration the sealing of sections of the surfaces close to the edges of the pressurized cavity and on the plane surfaces. The finite element mesh discretizations used to model the axisymmetric hydraulic pulse test are identical to those used previously to examine the transient purely radial flow problem. Figure 4 compares the decay curves associated with purely radial flow to the actual boundary condition. The computational results indicate that the analytical solution (Equation 5) for the infinite domain problem adequately describes the transient decay of the pressure pulse in the laboratory experiment.

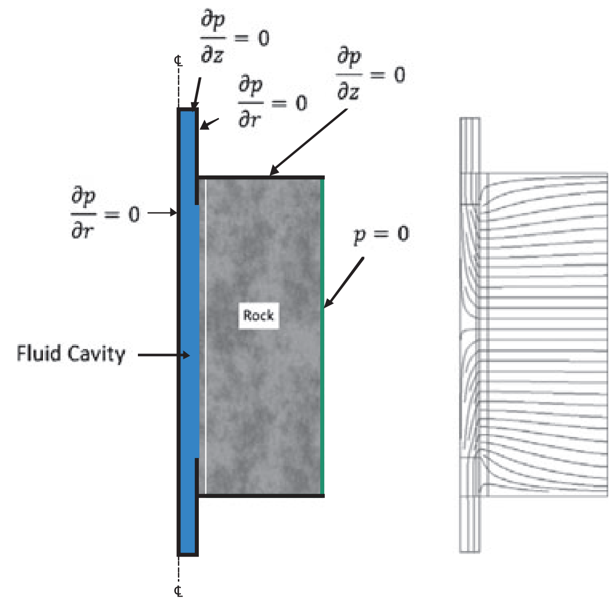

Figure 3. Boundary condition and flow pattern during laboratory testing.

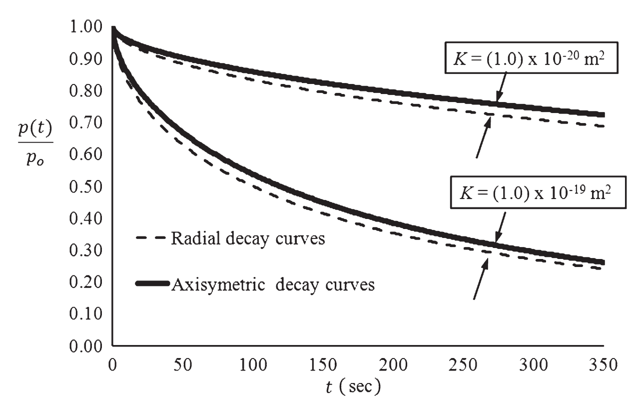

Figure 4. Comparison of pressure pulse decay in tests conducted under radially symmetric and axisymmetric flow conditions.

Experimental Results and Interpretation

In this section, we briefly summarize the results of the relevant tests on the four samples and interpret the permeability of the Lindsay limestone derived from the results. Details relating to steady-state and transient tests results are given by Jenner (2011).

Steady-State Tests

A series of steady-state tests was conducted on the four cylindrical samples of the Lindsay limestone; 4 tests were performed on Sample 1, 10 tests on Sample 2, and 6 tests on Sample 3 and the DGR Site Core. The Quizix precision pump was used to apply a constant pressure to the central cavity and to measure the changing flow rate. Typical examples of the constant pressure test results for Samples 1 and 2 are given in Figure 5a and 5b respectively. In both tests, the flow rate through the sample shows variability with time, commencing with a higher flow rate that decreases when steady state is achieved. Figure 5a and 5b also illustrates the order of magnitude difference in permeability between the two samples. Several steady-state permeability tests were conducted at

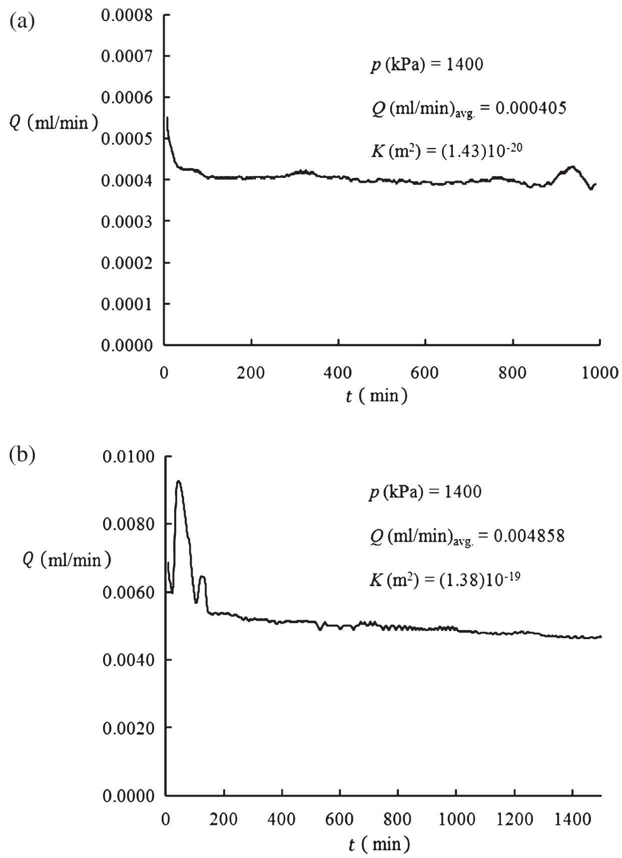

Figure 5. Steady-state 1400-kPa constant pressure test results for Samples (a) 1 and (b) 2.

internal pressures varying from 200 to 2000 kPa. Each steady-state flow test lasted between 250 min and 8 d.

For Sample 1, the permeability estimates determined from constant pressures, between 1000 and 1400 kPa, ranged from 1.17×10^{-20} to 4.98×10^{-20} m^2. For Sample 2, the estimated permeability ranged from 1.38×10^{-19} to 1.68×10^{-19} m^2 under constant pressures between 400 and 1800 kPa. For Sample 3, the estimated permeability ranged from 6.2×10^{-21} to 9.0×10^{-21} m^2, under constant pressures between 200 and 1600 kPa. For the DGR Site Core, the estimated permeability estimates ranged from 1.0×10^{-22} to 5.25×10^{-21} m^2, under constant pressures between 200 and 2000 kPa. The range of permeability values in the horizontal plane reported by Vilks and Miller (2007) and Gartner Lee Ltd. (2008) were between 1.22×10^{-22} and 4.08×10^{-18} m^2 and the data from the present investigations are bounded by these values. It is noted that during all the steady-state tests performed, a slow almost linear decrease in the permeability was observed. When the fluid is injected at a constant pressure, the permeability is expected to decrease with time until the pressure effects reach the outer boundary of the cylinder and the hydraulic gradient eventually becomes constant. This is evident in Figure 5b where the flow rate decreased gradually between 200 and 1400 min under the application of a constant pressure of 1400 kPa. This type of phenomenon was reported by Jacob and Lohman (1952) and is also evident in steady-state tests documented by Selvadurai et al. (2005) and Selvadurai and Glowacki (2008).

Transient Hydraulic Pulse Tests

Transient hydraulic pulse tests were conducted on Samples 2, 3, and the DGR Site Core. The pressure pulses were of 350 s duration. Cavity pressures applied during these tests were well below the pressures needed to initiate delamination of the epoxy bonding on either the Lindsay limestone or the fittings. Using the supplied "Pumpworks" software, a flow rate of between 0.2 and 1 mL/min was applied to the fluid-filled cavity initially maintained at atmospheric pressure. The cavity pressure was allowed to increase to the desired level at which time the inlet valve was closed. The time required to attain the pressure pulses ranged from 2 to 8 s. This is not a precise definition of the Dirac delta function-type pressure rise associated with the analytical result, but the procedure is considered sufficient for the purpose of application of the analytical result (Equation 5) and to limit the development of excess pressure fields in the flow domain. In computational treatments, however, the precise pressure history applied to the cavity can be matched and comparisons between the two results can be used to better define the pressurizing field induced within the fluid-saturated rock at the start of the pulse test.

As has been shown by Selvadurai (2009), residual pressure fields can influence the time history of the pressure decay within the cavity. For this reason, sufficient time was allowed between the tests to permit the dissipation of residual pressures. Computational simulations (based on a lower bound for the permeability of the Lindsay limestone) of the decay of the residual pressure fields indicate that approximately a 2-h interval between tests is sufficient to allow for complete dissipation of the residual pressure. The procedure for estimation involves the matching of the experimental data with computational estimates where the following parameters were fixed: $C_w = 4.54 \times 10^{-7}$ m^2/kN; $C_{eff} = 7.22 \times 10^{-8}$ m^2/kN; $n^* = 0.01$; $\gamma_w = 988.08$ kg/m^3; and $\mu = 0.000979$ kg/m s. The compressibility of the porous skeleton, C_{eff} was determined using

$$C_{eff} = \frac{3(1-2v)}{E} \tag{8}$$

where E and v were chosen as 20.8 GPa and 0.25, respectively, based on tests conducted at McGill University. The porosity was chosen as 0.01 to give conservative permeability results, although the estimated permeability change under a higher porosity value (e.g., $n = 0.034$) is negligible (Selvadurai et al. 2011; Jenner 2011). The pressure decay curves for the hydraulic pulse tests were computationally evaluated by assigning a range of values for the permeability.

The time-dependent decay of the pressure pulses within the pressurized cavity for the DGR Site Core is shown in Figure 6. The permeability is estimated to be between 1.25×10^{-21} and 2.0×10^{-21} m^2 for pressure pulses between 375 and 471 kPa. For Sample 2,

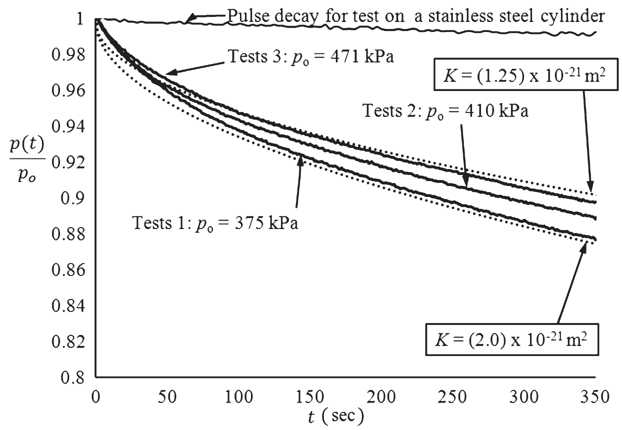

Figure 6. Experimental (solid line) and computational (dashed line) decay curves for Site Core, as well as pulse decay for test on a stainless steel cylinder.

at the lower range of cavity pulse pressures of 100 kPa, the permeability of the Lindsay limestone is estimated to be approximately 1.0×10^{-20} m^2, while at intermediate cavity pulse pressures (500 to 1200 kPa), the permeability is approximately 7.6×10^{-20} m^2. The experimental decay curves fit the computational decay curves better at the upper end of the cavity pressures (1658 to 1706 kPa), where the permeability is estimated to be between 1.30×10^{-19} and 1.50×10^{-19} m^2. For Sample 3, at cavity pulse pressures ranging between 191 and 316 kPa, the permeability of the Lindsay limestone is estimated to be between 1.0×10^{-21} and 2.0×10^{-21} m^2, while at cavity pulse pressures from 552 to 561 kPa, the permeability is estimated to be between 3.5×10^{-21} and 6.0×10^{-21} m^2. The influence of the cavity pressures on the estimated permeability suggests that hydraulic performance of the sample is influenced by the test procedure. A factor that could lead to an increase in the permeability during an increase in the pulse pressure is the opening of any discontinuities and defects due to tensile stress fields. A tensile stress field could be generated at the cavity boundary because of the hoop stresses associated with pressurization or because of the axial stress induced in the vicinity of the seals.

Conclusions

The permeability of Lindsay limestone is a critical component for assessing the feasibility of the proposed DGR in terms of radionuclude migration from the storage facility in the long term. The experimental approach presented, which involves the radial flow testing of a cylindrical specimen with an end-sealed cylindrical cavity, is an effective technique specifically geared for testing low permeability porous geomaterials. The permeability estimates obtained from the current series of experiments are between 1.0×10^{-22} and 1.68×10^{-19} m^2. These are within the range of previous results found in the literature. Both transient and steady-state test methods give similar permeability estimates. Differences in permeability between methods may be attributed to possible sources of error for the pulse tests results; incorrect estimates of C_{eff} or the presence of air within the cavity are thought to be two such factors. In addition, micro-mechanical damage that results in crack generation may have occurred due to sample drying, particularly in the argillaceous zones, or the influence of stress-relief and opening of fissures prior to testing. The Site Core, retrieved from a depth of 680 m, was completely sealed until the time of testing, whereas the samples from the quarry site were cored from block samples obtained from a depth of 80 m. The samples were *unconfined* during all tests. Axial tensile stresses, hoop stresses, and pore pressures can be influenced by the cavity pressure, which could increase the permeability values if the pressurization induces microcracking and damage. The average tensile strength was of the order of 1 MPa and the maximum cavity pressure applied to conduct the pulse tests was of the order of 0.5 MPa. The consistency of the results for the permeability would indicate that the samples remained relatively intact during permeability testing.

Acknowledgments

This work was supported by a Strategic Research Grant awarded by the Natural Sciences and Engineering Research Council of Canada and through a Research Grant awarded by the Nuclear Waste Management Organization (NWMO), Toronto, ON, both awarded to A.P.S.S. The authors are grateful to the research personnel at the NWMO, for their interest in the research. The block of Lindsay limestone was provided *by Saint Mary's Quarry*, Bowmanville Ontario, and the assistance of the Quarry coordinator, Mr. Nick Papanicolaou, is gratefully acknowledged. The authors are grateful to the staff of *Geofirma Engineering Limited* for providing samples of the DGR Site Cores. The assistance of Mr. John Bartczak, of the *Environmental Geomechanics Laboratory* at McGill University, is acknowledged. Finally, the authors gratefully acknowledge the valuable comments provided by Professor Frank W. Schwartz, Editor-in-Chief, *Ground Water* and the associate editor.

References

Alonso, E.E., T.S. Alcoverro, J. Armand, L. Borgesson, M. Chijimatsu, F. Coste, P. Jussila, M. Itamura, J. Hernelind, A. Ito, I. Kadiri, A. Kobayashi, H. Kurikami, F.L. Malinsky, Z. Maouche, V. Merrien-Soukatchoff, V. Nguyen, T. Nowak, A. Rejeb, J. Rutqvist, H. Shao, S. Sobolik, C. Stone, Y. Sugita, M. Tijani, C.-F. Tsang, A.P.S. Selvadurai, and S.W. Webb. 2005. The FEBEX benchmark test: Case definition and comparison of modeling approaches. *International Journal of Rock Mechanics and Mining Sciences* 42: 611–638.

Bachu, S., and J.J. Adams. 2003. Sequestration of CO_2 in geologic media in response to climate change: Capacity of deep saline aquifers to sequester CO_2 in solution. *Energy Conversion and Management* 44: 3151–3175.

Barenblatt, G.I., V.M. Entov, and V.M. Ryzhik. 1990. *Theory of Fluid Flows through Natural Rocks.* Dordrecht, The Netherlands: Kluwer Academic Publishers.

Bear, J., C.-F. Tsang, and G. de Marsily. 1993. *Flow and Contaminant Transport in Fractured Rock.* San Diego: Academic Press.

Bernaix, J. 1969. New laboratory methods of studying the mechanical properties of rocks. *International Journal of Rock Mechanics and Mining Sciences* 6: 43–89.

Brace, W.F., J.B. Walsh, and W.T. Frangos. 1968. Permeability of granite under high pressure. *Journal of Geophysical Research* 73: 2225–2236.

Bredehoeft, J.D., and S.S. Papadopulos. 1980. A method for determining the hydraulic properties of tight formations. *Water Resources Research* 16: 233–238.

Bredehoeft, J.D., H.H. Cooper, and S.S. Papadopulos. 1966. Inertial and storage effects in well-aquifer systems: An analogue investigation. *Water Resources Research* 2: 697–707.

Carslaw, H.S., and J.C. Jaeger. 1959. *Conduction of Heat in Solids.* Oxford: Oxford University Press.

Chapman, N.A., and I.G. McKinley. 1987. *The Geological Disposal of Nuclear Waste.* New York: John Wiley and Sons.

Cooper, H.H., J.D. Bredehoeft, and S.S. Papadopulos. 1967. Response of a finite-diameter well to an instantaneous charge of water. *Water Resources Research* 3: 263–269.

Daw, G. 1971. A modified Hoek-Franklin triaxial cell for rock permeability measurements. *Revue Francaise Geotechnique* 21: 89–91.

Ferris, J.G., D.B. Knowles, R.H. Brown, and R.W. Stallman. 1962. Theory of aquifer tests. *US Geological Survey Water Supply Paper.*

Gartner Lee Limited. 2008. DGR Supporting Technical Report: Phase I Geosynthesis. *Report to Ontario Power Generation*. 00216-REP-01300-00010-R00 (DOC 556).

Golder Associates. 2003. Low level waste geotechnical feasibility study—western waste management facility Bruce Site, Tiverton, Ontario. *Report to Ontario Power Generation*.

Hearn, N., and R.H. Mills. 1991. A simple permeameter for water or gas flow. *Cement and Concrete Research* 21: 257–261.

Heystee, R., and J.C. Roegiers. 1981. The effect of stress on the primary permeability of rock cores - A facet of hydraulic fracturing. *Canadian Geotechnical Journal* 21: 257–261.

Hsieh, P.A., J. Tracy, C. Neuzil, J. Bredehoeft, and S. Silliman. 1981. A transient laboratory method for determining the hydraulic properties of 'tight' rocks - I. Theory. *International Journal of Rock Mechanics and Mining Sciences and Geomechanics Abstracts* 18, no. 3: 245–252.

Jacob, C.E., and S.W. Lohman. 1952. Nonsteady flow to a well of constant drawdown in an extensive aquifer. *Transactions of the American Geophysical Union* 33, no. 4: 559.

Jenner, L. 2011. Radial hydraulic flow testing of an argillaceous limestone. Master thesis, Department of Civil Engineering and Applied Mechanics, McGill University, Montreal QC.

Lam, T., D. Martin, and D. McCreath. 2007. Characterising the geomechanics properties of the sedimentary rocks for the DGR excavations. *Report to Ontario Power Generation*.

Mazurek, M. 2004. Long-term used nuclear fuel waste management—geoscientific review of the sedimentary sequence in Southern Ontario. *Technical Report TR 04-01*, Institute of Geological Sciences, University of Bern, Bern, Switzerland.

Muskat, M., and R.W. Wyckoff. 1946. *The Flow of Homogeneous Fluids through Porous Media.* Ann Arbor, Michigan: J.W. Edwards, Inc.

Raven, K., K.S. Novakowski, R.M. Yager, and R.J. Heystee. 1992. Supernormal fluid pressures in sedimentary rocks of southern Ontario: Western New York State. *Canadian Geotechnical Journal* 29: 80–93.

Selvadurai, A.P.S. 2009. Influence of residual hydraulic gradients on decay curves for one-dimensional hydraulic pulse tests. *Geophysical Journal International* 177: 1357–1365.

Selvadurai, A.P.S. 2006. Gravity-driven advective transport during deep geological disposal of contaminants. *Geophysical Research Letters* 33: L08408. DOI: 10.1029/2006GL025944.

Selvadurai, A.P.S. 2002. Influence of pressurized water influx on the hydro-thermal behaviour of an engineered clay barrier in a waste emplacement borehole. *Engineering Geology* 64: 157–178.

Selvadurai, A.P.S. 2000. *Partial Differential Equations in Mechanics Volume 1: Fundamentals, Laplace's Equation, Diffusion Equation, Wave Equation.* Berlin: Springer-Verlag.

Selvadurai, A.P.S., and P.A. Selvadurai. 2010. Surface permeability tests: experiments and modeling for estimating effective permeability. *Proceedings of the Royal Society, Mathematics and Physical Sciences, Series A* 466: 2819–2846.

Selvadurai, A.P.S., and A. Glowacki. 2008. Permeability hysteresis of limestone during isotropic compression. *Ground Water* 46: 113–119.

Selvadurai, A.P.S., and P. Carnaffan. 1997. A transient pressure pulse method for the measurement of permeability of a cement grout. *Canadian Journal of Civil Engineering* 24: 489–502.

Selvadurai, A.P.S., and T.S. Nguyen. 1996. Scoping analyses of the coupled thermal-hydrological-mechanical behaviour of the rock mass around a nuclear fuel waste repository. *Engineering Geology* 47: 379–400.

Selvadurai, A.P.S., A. Letendre, and B. Hekimi. 2011. Axial flow hydraulic pulse testing of an Argillaceous Limestone. *Environmental Earth Sciences* 64: 2047–2058.

Selvadurai, A.P.S., M.J. Boulon, and T.S. Nguyen. 2005. The permeability of an intact granite. *Pure and Applied Geophysics* 162: 373–407.

Selvadurai, P.A. 2010. An approach for modeling hydraulic pulse tests using finite element techniques (*Personal Communication*).

Selvadurai, P.A., and A.P.S. Selvadurai. 2007. On cavity flow permeability testing of a sandstone. *Ground Water* 45: 93–97.

Thiem, G. 1906. *Hydrologische Methoden (Hydrologic Methods).* Leipzig: J.M. Gebhardt.

Trimmer, D., B. Bonner, H. Heard, and A. Duba. 1980. Effect of pressure and stress on water transport in intact and fractured Gabbro and Granite. *Journal of Geophysical Research* 85: 7059–7071.

Vilks, P., and N.H. Miller. 2007. *Evaluation of Experimental Protocols for Characterizing Diffusion in Sedimentary Rocks, Nuclear Waste Management Division Report TR-2007-11.* Toronto, ON: Atomic Energy of Canada Limited.

White, F.M. 1986. *Fluid Mechanics*, 2nd ed. New York: McGraw Hill.